2012 IEEE/RSJ International Conference on
Intelligent Robots and Systems
October 7-12, 2012. Vilamoura, Algarve, Portugal

# Exploiting Passive Dynamics for Robot Throwing Task

Robin Thandiackal, Christoph Brandle, Derek Leach, Amir Jafari* and Fumiya Iida

*Abstract*— **Throwing is a complex and highly dynamic task. Humans usually exploit passive dynamics of their limbs to optimize their movement and muscle activation. In order to approach human throwing, we developed a double pendulum robotic platform. To introduce passivity into the actuated joints, clutches were included in the drive train. In this paper, we demonstrate the advantage of exploiting passive dynamics in reducing the mechanical work. However, engaging and disengaging the clutches are done in discrete fashions. Therefore, we propose an optimization approach which can deal with such discontinuities. It is shown that properly engaging/disengaging the clutches can reduce the mechanical work of a throwing task. The result is compared to the solution of fully actuated double pendulum, both in simulation and experiment.**

## I. INTRODUCTION

Throwing is a highly dynamic task. The action of throwing needs synchronized movements in the sequence of stride, hip rotation, trunk rotation, and arm movement. When executing such tasks, animals and humans, through the necessity of evolutionary fitness, have optimized their movement and muscle activation to minimize energy consumption and strain on joints and tissues. The consequences of this optimization are graceful movements that make extensive use of the passive dynamics inherent in the body and its interaction with the environment [1], [2]. Humans also adopt methods to speed up the optimization of the complex movements. Bernstein [3] suggested that when learning complex high dimensional tasks, humans at first restrict or freeze redundant degrees of freedom to simplify the learning process and then gradually release them as they become more skilled at the task. In this way the optimization process is guided to a solution much more rapidly. Such a process has been observed in a number of studies, [4], [5].

In order to approach the human throwing, we developed a simple yet representative double pendulum platform that can capture the main parts of the dynamical behaviour. Inspired by the importance of passivity in human actions, we include electromagnetic clutches in the drive train to introduce passivity into the actuated joints. Some recent research has studied throwing task numerically and experimentally. For instance, high-speed throwing motion was presented by Senoo et al [6] for a 3-degree-of-freedom (DOF) human-like arm with full actuation. The aim was to reach high velocities at the elbow motivated by the high speed of up to 40 rad/s at low torque that exist in human sports activities such as baseball pitching [7]. Another related study is of a golf-swing robot [8]. This robot can perform human-like golf swings with a specified hitting speed at a certain impact position. Birglen et al presented an encompassing optimization study for under-actuated mechanisms [9], focusing mainly on four-bar linkages but with applications to other transmission mechanisms as well. Four-bar linkages were also used in [10] and [11]. These studies have led to the construction of remarkably efficient hands and arms [12].

Although there are some previous attempts to exploit passive dynamics for robotic throwing motions, the use of clutch mechanisms has not been explored in the robotic systems. While clutches are one of the most well-established mechanical components, the control of trajectories becomes a challenging problems as soon as they are employed in the robotic joints. In general, agile motions are feasible using passive or under-actuated mechanisms. However, the task of motion planning and control design are extremely challenging due to arising differential and even discrete constraints that restrict the class of feasible motions.

From this perspective, the goal of this paper is to propose an approach to deal with the discontinuities induced by the clutches for efficient throwing motions. For a systematic analysis, we employ a simple double pendulum which equips with two clutches in series to electromagnetic motors in both of the rotational joints. By using this setup, we demonstrate that the online switching between active and passive through the clutches can result in reduced mechanical work compared to the solution of fully actuated double pendulum.

In Section II the throwing task of the double pendulum is modeled, Section III presents a control method that is able to optimize a system with discontinuities. Simulation results are presented in section IV. Finally Sections V and VI show

* This study was supported by the Swiss National Science Foundation Grant No. PP00P2123387/1, and the Swiss National Science Foundation through the National Centre of Competence in Research Robotics.Robin Thandiackal, Christoph Bra¨ndle, Derek Leach, Amir Jafari and Fumiya Iida are with the Department of Mechanical and Process Engineering, Swiss Federal Institute of Technology Zurich, 8032 Zurich, Switzerland. Corresponding author: Amir Jafari [ajafari@ethz.ch].

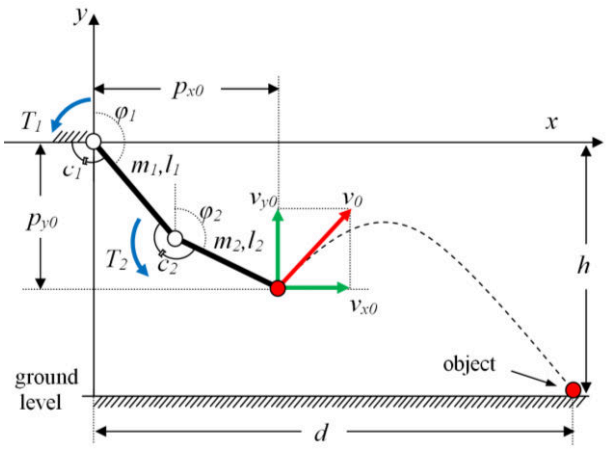


Fig. 1. Modeling of throwing an object by the double pendulum.

experimental results on the double pendulum robot and provide conclusions, respectively.

## II. Modeling of the Throwing Task

Throwing an object using the double pendulum consists of two consequent phases. The first phase is before releasing the object until the double pendulum reaches the configuration shown in Fig.1. The second phase starts after the object is released and finishes when the object hits the ground. Therefore, to analyze the task, the dynamics of the double pendulum in the first phase as well as the ballistic motion of the thrown object during the second phase have to be modeled.

### A. Double Pendulum Dynamics

The pendulum is modeled as two links with masses, $m_1$ and $m_2$, and two link inertias, $I_1$ and $I_2$. Furthermore, damping is introduced into the joints with the corresponding damping coefficients as $c_1$ and $c_2$.

The equations governing the system can be written as:

$$M(q)\ddot{q} + D\dot{q} + C(q,\dot{q}) + G(q) = \tau \qquad (1)$$

where $q=[\varphi_1\ \varphi_2]^T$ is the vector of joint angles and $\tau=[T_1\ T_2]^T$ is a vector of the motor torques. $M$ is the mass matrix, $D$ is a matrix containing joint damping terms, $C$ is a vector containing Coriolis effects and $G$ is a vector of gravitational forces. The unknown parameters $I_1$, $I_2$, $c_1$ and $c_2$ can be found via a system identification procedure which is explained in section V. Engaging and disengaging the clutches dramatically changes the damping coefficients of the joints. Therefore, two actuation modes, namely active and passive, are considered for each joint. The active mode is when the clutch is engaged while disengaging the clutch switches the mode to the passive one.

### B. Ballistics Projectile Model

The thrown object in the second phase has a ballistic motion. We do not intend to predict the throwing distance with high accuracy. Therefore, only the gravitational effects are considered and aerodynamic resistance is neglected. Using the coordinate system defined in Fig. 1, the throwing distance can be computed as follow:

$$d(p_0, v_0) = p_{x0} + \frac{v_{x0}}{g}\left[v_{y0} + \sqrt{2g\left(h + p_{y0}\right) + v_{y0}^2}\right] \qquad (2)$$

where $g$ is the gravitational acceleration, $p_0=[p_{x0}\ \ p_{y0}]^T$ is the cartesian release position, $v_0=[v_{x0}\ \ v_{y0}]^T$ is the cartesian release velocity. The ground surface is assumed to be at $y=-h$. As the release parameters result from the double pendulum dynamics, it is useful to convert $p_0$ and $v_0$ into the corresponding angular coordinate $q$.

$$p_0 = \begin{bmatrix}\sin(\varphi_1^*) & \sin(\varphi_2^*)\\ \cos(\varphi_1^*) & \cos(\varphi_2^*)\end{bmatrix} l$$

$$v_0 = \begin{bmatrix}\dot{\varphi}_1^*\sin(\varphi_1^*) & \dot{\varphi}_2^*\sin(\varphi_2^*)\\ -\dot{\varphi}_1^*\cos(\varphi_1^*) & -\dot{\varphi}_2^*\cos(\varphi_2^*)\end{bmatrix} l \qquad (3)$$

where $l=[l_1\ \ l_2]^T$ and $(.)^*$ indicates angles and angular velocities at release. By using (2) and (3) one can finally rewrite equation (2) as:

$$d(p_0, v_0) = d(q^*, \dot{q}^*). \qquad (4)$$

## III. Optimization Approach

The goal of optimization is to minimize the mechanical work required to throw an object to a desired distance $d_{des}$. The optimization approach, however, can deal with switching between the active and the passive modes at each joint. This considerably increases the computation time to find an optimal solution. Therefore, to simplify the optimization process, the trajectory of the first link is considered to be fixed. The following subsections discuss essentials of the optimization approach.

### A. Simplification of optimization problem

To simplify the problem, here we consider to fix the first link trajectory:

$$\begin{aligned}\dot{x}(t) &= f(x(t), \varphi_1(t), T_2(t))\\ T_1(t) &= h(x(t), \varphi_1(t), T_2(t))\end{aligned} \qquad (5)$$

where $x(t)=[\varphi_2(t)\ \ \dot{\varphi}_2(t)]^T$.

Given the system dynamics in (5), the goal is to find the control inputs $T_1$ and $T_2$ such that the desired throwing distance $d_{des}$ can be reached in an energy efficient way.

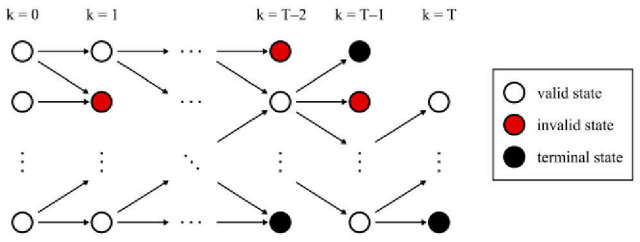


Fig. 2. Graph construction

### B. Discretization

The immediate change between the active and the passive modes produces discontinuities. Therefore, to solve the problem, it is reasonable to focus on a discrete state space. The system dynamics can then be described by state transitions. This allows discontinuities in the model to be easily incorporated. Consequently, the optimal state sequence can be found through dynamic programming.

In addition to the time discretization, we also introduced a spatial discretization as follow:

$$\begin{aligned} x[k+1] &= x[k] + f(x[k], \varphi_1(k\Delta t), T_2[k])\Delta t \\ T_2[k+1] &= T_2[k] + u[k] \\ T_1[k+1] &= h(x[k], \varphi_1(k\Delta t), T_2[k]) \end{aligned} \tag{6}$$

where $x[k]$ and $T_2[k]$ are the states and $u[k] \in [-u_{max}, 0, u_{max}]$ is the input. $\Delta t$ describes the sample time and $k$ indicates the discrete time at t = kΔt.

### C. Terminal states

The terminal states determine when a trajectory is finished. In this problem, the terminal states describe the release position and velocity which lead to the desired throwing distance $d_{des}$.

### D. State transition

At each time step, depending on the current state and the chosen input, several next states can be reached (Fig 2). However, there are some invalid states which violate some constraints such as the torque limit of the clutches.

Therefore, before applying an optimization algorithm, these states and all the paths which do not lead to a terminal state have to be excluded. The remaining graph then consists of solution trajectories. A solution trajectory is a path from an initial state to a terminal state.

### E. Cost function

In the dynamic programming framework, the total cost of a solution trajectory is defined as the sum of costs of all state

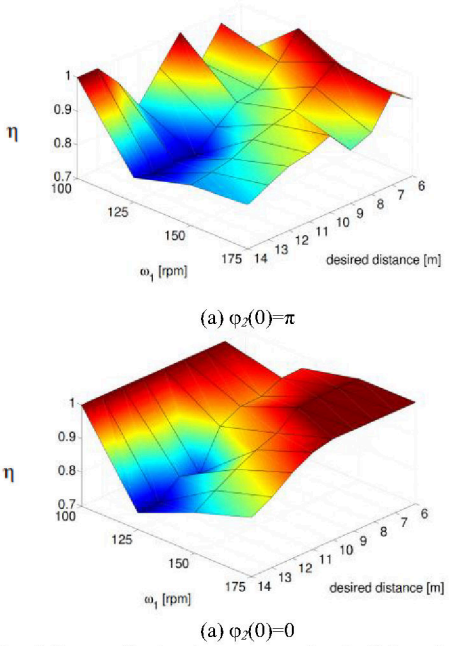


(a) $\varphi_2(0)=\pi$

(a) $\varphi_2(0)=0$

Fig. 3. Simulation results showing energy ratios for fully active and active-passive throwing for different first link trajectories and desired throwing distances, result for initial position of the second link :(a) bottom dead center (b) top dead center.

transitions within a solution trajectory. Such a cost increment is defined through the cost function $g$. The optimization process should minimize the total mechanical work. Therefore, $g$ is defined as the mechanical work needed to reach from a current state at time $k$ to the next state at time k +1.

$$\begin{aligned} g(\varphi_1(t), x_1[k], T_2[k]) &= |T_1[k]\Delta\varphi_1| + |T_2[k](\Delta\varphi_1 - \Delta\varphi_2)| \\ \Delta\varphi_1 &= \varphi_1((k+1)\Delta t) - \varphi_1(k\Delta t) \\ \Delta\varphi_1 &= x_1[k+1] - x_1[k] \end{aligned} \tag{7}$$

The optimal solution is therefore the path from a certain initial state at $k=0$ to a terminal state, such that the total cost is minimized.

### F. Value Iteration

Finally, to solve the discrete optimal control problem, the dynamic programming algorithm is used. As this problem is an infinite horizon problem (no termination time), the algorithm leads to *Bellman*'s equation for the optimal cost. An appropriate method to find the solution in this case, is the Value Iteration algorithm [13]. It guarantees convergence to the optimal cost to go from each state to the terminal state. The algorithm is formulated as follows:

$$J_{n+1}(i) = \min_u (g(i,u) + \sum_j p_{ij}(u) J_n(j)) \quad \forall i \tag{8}$$

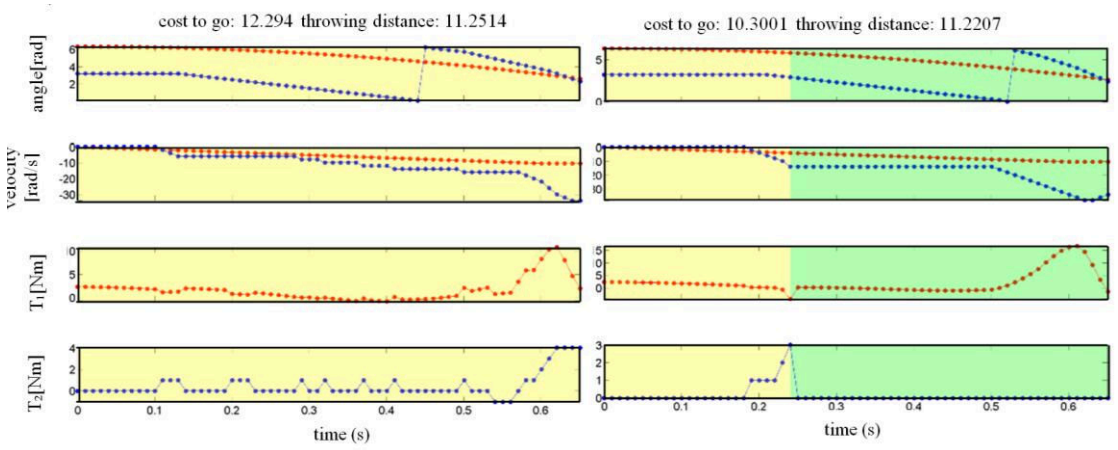


Fig. 4. Optimal control solution for $\omega_1$=100rpm and desired distance of 11 m, initial condition of second link $\varphi_2(0)=\pi$. First link data points in red, second link data points in blue. Green background indicates passive mode, thus clutches are disengaged.

where *i, j* represent the state at step *k* and *k +1*, respectively. *n* is the iteration number. *J(i)* is the cost to go from state *i* to the terminal state. *g* is the cost to go from state *i* to *j* by the input *u*. *p* is the probability of reaching state *j* from state *i* through applying the input *u*. As we are dealing with a deterministic problem:

$$\begin{aligned} p_{ij}(u) &= 1 \qquad for\ j = \hat{j} \\ p_{ij}(u) &= 0 \qquad for\ j \neq \hat{j} \end{aligned} \tag{9}$$

where $\hat{j}$ is the state that is reached from i by applying u. The sequence $J_n(i)$ converges to the optimal cost $J^*(i)$.

## IV. Simulation Results

To evaluate the performance of the optimization approach, the mechanical work required for a throwing task is calculated through the simulation. To show the effect of passive dynamics on reducing the mechanical work, two throwing scenarios are considered. In the first scenario, which is called fully active throw, the clutch is engaged all the time. The second scenario is active-passive throw and it allows disengaging of the clutch during execution of the task. However, the following constraints from the real world platform are also considered in the simulation:

1- Switching between modes is only allowed from active to passive not the other way round.

2- While the clutches are engaged, the torques $T_1$ and $T_2$ are restricted due to the torque limits of the clutches and motors.

$$T_i \in [-T_{i,\max}, T_{i,\max}] \quad i = 1,2 \tag{10}$$

As it was mentioned in the section III, the first link trajectory is pre-defined. In order to select a proper trajectory for the first link, we assume that the first link starts at top dead center $\varphi_1(t_0)=0$ with zero velocity and constant acceleration. Then it moves by zero acceleration and constant velocity after passing through bottom dead center $\varphi_1(t)=\pi$. Such a trajectory is easy to handle, smooth and needs only the bottom velocity $\omega_1$ for unique parameterization. The trajectory is given by means of the following equations.

$$\begin{aligned} \varphi_1(t) &= -\frac{\omega_1^2}{4\pi}t^2 \\ \dot{\varphi}_1(t) &= -\frac{\omega_1^2}{2\pi}t \end{aligned} \quad \Big| \quad for\ \varphi_1(t) > -\pi$$

$$\begin{aligned} \varphi_1(t) &= -\omega_1 t \\ \dot{\varphi}_1(t) &= -\omega_1 \end{aligned} \quad \Big| \quad for\ \varphi_1(t) \le -\pi \tag{11}$$

With the first link trajectory fixed, the second link can be controlled in either fully active or active-passive fashion. The value iteration method can then lead to a solution trajectory for each of these cases. The active-passive solution is derived with results from an extended graph (section III-D). This is because each node of the graph includes additional possibility to switch to the passive mode. The corresponding mechanical works ($W_{fully\ active}$, $W_{active\text{-}passive}$) are then calculated through the cost function. Therefore an energy saving measure $\eta$ can be defined as:

$$\eta = \frac{W_{active-passive}}{W_{fully active}} \tag{12}$$

Fig. 3 shows the ratio of energy between the active-passive and active throws for a number of different parameters. The plots show that especially for larger desired distances energy saving is more significant. The simulation result also shows that for different initial conditions of the second link the energy saving varies. With the initial state of

Table I. Identified parameters

| Parameters | Modes | |
|---|---|---|
| | *Active* | *Passive* |
| $I_1[Kgm^2]$ | 0.01 | 0.01 |
| $I_2[Kgm^2]$ | 0.003 | 0.0009 |
| $c_1[Nms]$ | 0.037 | 0.004 |
| $c_2[Nms]$ | 0.14 | 0.03 |
| $m_1[Kg]$ | 0.7 | 0.7 |
| $m_2[Kg]$ | 0.8 | 0.8 |
| $l_1[m]$ | 0.3 | 0.3 |
| $l_2[m]$ | 0.2 | 0.2 |

the second link around $\varphi_2(t_0)=\pi$ the energy saving is greater than that with the initial state around $\varphi_2(t_0)= 0$. Figs. 4-a and 4-b show an example of solution trajectories and corresponding torque for fully active and active-passive throwing, respectively.

## V. Implementation into Double Pendulum Robot

We developed a planar double pendulum robot to test the feasibility of the method in the real world. To test whether the trajectories produced with the method presented in Section III would also yield improved performance in a physical system, we developed a planar double pendulum robot. Two electromagnetic toothed clutches are included at the shoulder and elbow joints. The experimental set-up can be seen in Fig. 5. Two Maxon RE 40 DC motors with 15:1 planetary gear reduction were used to drive the two degrees of freedom, and each motor was connected in series with a Miki Pulley 546-12-34NF electromagnetic toothed clutch. The clutches have a maximum permissible torque of 17.5 Nm and weigh 0.5 kg. Both motors are mounted along the same axis of the elbow and shoulder joints. The elbow motor is located at the shoulder but it drives the elbow joint via a toothed belt to reduce the inertia of the links. A Maxon EPOS2 motor controller was used for each motor. The trajectories were implemented using the in-built cubic interpolated position mode of EPOS2. In order to validate the feasibility of the approach, system parameters have to be identified. For the parameter identification, the physical double pendulum is released at the position $q=[\pi/2\ \pi/2]^T$. Then with the motors switched off the trajectory of the link angles is recorded. In simulation the model is then fitted to the measurement, where we use *fminsearch*. The chosen release position is selected because we can expect a smooth and repeatable swinging motion where especially damping is adequately visible. The absolute values of the parameters are listed in Table I. The system behaviour strongly depends on whether the clutches are engaged or disengaged. We then perform a completely passive throw to validate the identified parameters. In the passive throw, both clutches are disengaged. The double pendulum starts from a given initial configuration and throws the object. In this case, we only need to define the initial joint angles and set the initial joint torques ($T_1$ and $T_2$) and velocities ($\dot{\varphi}_1$ and $\dot{\varphi}_2$) to zero. The model (1) is simulated for

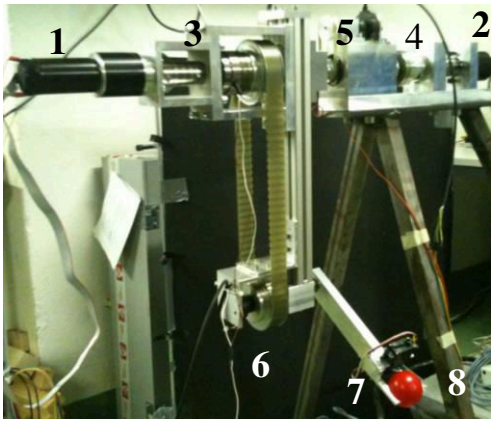


Fig. 5. Hardware setup of double pendulum: 1 Elbow motor , 2 Shoulder motor, 3 Elbow clutch, 4 Shoulder clutch, 5 Elbow hall sensor, 6 Shoulder hall sensor, gripper 7 and the object 8.

discrete set of initial angles ($\varphi_i$ [0.2π), $i$= 1,2, is mapped to a discrete interval of 300 points). For each particular initial condition, the simulation provides a trajectory. The throwing distance is calculated for each time step and the maximum distance for each trajectory is selected. This allows us to find the best release position of the object with the corresponding maximum distance for each trajectory, and therefore each initial condition. The results are shown in Fig. 6. The graph shows two regions where initial conditions consistently throw large distances, the region around ($\varphi_1$ , $\varphi_2$)=(-0.1, -π/2) (labeled A) and the region around ($\varphi_1$, $\varphi_2$)=(-π/4, π/4) (labeled B). The trajectories resulting from the two regions have their own characteristic behaviour. Fig. 7 qualitatively shows the trajectories arising from the two regions. For region A (Fig. 7-a) the second link always turns in the same direction (CW) and completes more than one full revolution before release. From region B (7-b) the second link turns CCW in the beginning and then changes direction to CW. Interestingly, similar characteristics have been encountered in the solutions of the fully active and active-passive throws. Having a closer look at the trajectories of the fully active and active-passive cases, we can observe that the optimal energy solutions share significant characteristics with the best solutions from the completely passive throw. For second link initial conditions around $\varphi_2(0)=\pi$ the solution tends to a motion resembling region-A trajectories (one full turn of link 2) whereas second link initial conditions with a similar angle to $\varphi_2(0)=0$ tend to region-B trajectories (half a turn of link 2). Especially the fact that the actuated energy efficient solution also mimics the behaviour from the completely passive solution strengthens the tie between energy minimization and passivity. In the simulation, the parameters $\Delta\varphi_2$, $\Delta\dot{\varphi}_2$ and $u_{max}$ are set as 0.1rad, 0.2 rad/s and 1N/m, respectively. The sampling time is 0.01s .One of the example trajectories in the simulation is then implemented on the double pendulum robot. The trajectories are computed off-line. The experiments give us qualitative

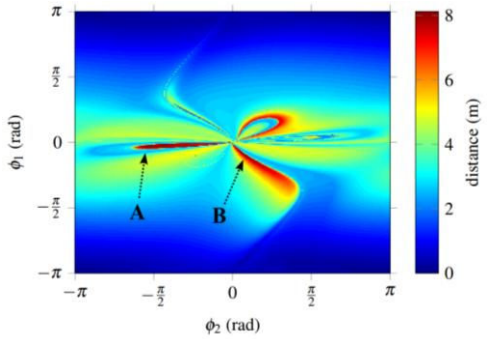


Fig. 6. Throwing distance in the passive throw as a function of initial joint angles.

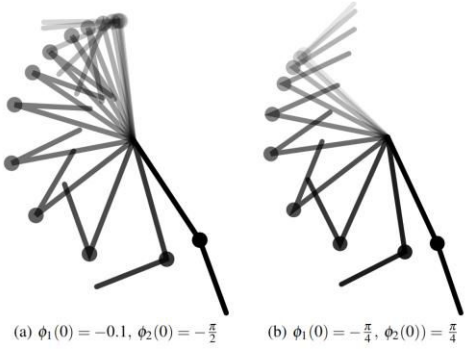


Fig. 7. Passive throw in stroboscopic view for two characteristic initial conditions leading to large thrown distances. The time between two captures is 0.05s

results in terms of energy and thrown distance. To derive the mechanical work, torque (from current measurement) and angle differences (hall sensors) were integrated.

To evaluate the mechanical work for fully active and active-passive throw, ($\omega_1$=100rpm and $\varphi_2(0)=\pi$), experiment has been carried out as follows: 20 runs for each case were performed. From these 20 runs those measurements which were consistent in terms of thrown distance are evaluated with respect to mechanical work. The latter is then represented through average value and standard deviation. As a result, in fully active mode 10 measurements were considered, whereas only 2 measurements were consistent in active-passive mode. The fully active scenario required 30.84+/-10.29J while the active-passive one accomplished the task by only 16.67+/-4.37J.The results clearly show that the active-passive throw needs less mechanical work. Finally, Fig. 8 shows a comparison between the computed and a resulting trajectory for the implemented active-passive throw.

## VI. Conclusion and Future Works

We presented a framework that is able to handle the inherent discontinuities arising from actuating joints with clutches. Simulation results as well as experiments on the double pendulum robot have shown that it is reasonable to use passive dynamics in order to reduce the mechanical work of a throwing task.

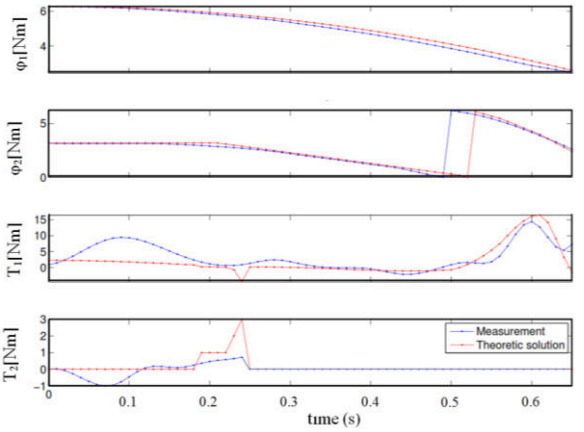


Fig. 8. Experimental Results: Measurement vs Theoretic solution of active-passive throw for $\omega_1$=100rpm and $\varphi_2(0)=\pi$. The clutch is disengaged at t = 0.25s

Finally, we indicated a positive interdependency between passivity and energy minimization. For the future works, we are aiming include the first link trajectory in the optimization process.

## References


[1] K. Schneider, R. F. Zernicke, R. A. Schmidt, and T. J. Hart, "Changes in limb dynamics during the practice of rapid arm movements," Journal of Biomechanics, vol. 22, no. 8–9, pp. 805–817, 1989.

[2] D. Debicki, P. Gribble, S. Watts, and J. Hore, "Kinematics of wrist joint flexion in overarm throws made by skilled subjects," Experimental Brain Research, vol. 154, no. 3, pp. 382–394, 2004.

[3] N. A. Bernstein, The Co-ordination and Regulation of Movements. Oxford, England: Pergamon Press, 1967.

[4] J. J. Buchanan and J. A. Kelso, "To switch or not to switch: Recruitment of degrees of freedom stabilizes biological coordination." Journal of motor behavior, vol. 31, no. 2, pp. 126–144, June 1996.

[5] J. Konczak, H. Vander Velden, and L. Ja¨ger, "Learning to play the violin: Motor control by freezing, not freeing degrees of freedom," Journal of Motor Behavior, vol. 41, no. 3, pp. 243–252, 2009.

[6] T. Senoo, A. Namiki, and M. Ishikawa, "High-speed throwing motion based on kinetic chain approach," in IEEE/RSJ International Conference on Intelligent Robots and Systems (IROS), Nice, France, September 2008, pp. 3206–3211.

[7] S. L. Werner, G. S. Fleisig, C. J. Dillman, and J. R. Andrews, "Biomechanics of the elbow during baseball pitching." The Journal of orthopaedic and sports physical therapy, vol. 17, no. 6, pp. 274–278, June 1993.

[8] C. Xu, A. Ming, T. Nagaoka, and M. Shimojo, "Motion control of a golf swing robot," Journal of Intelligent & Robotic Systems, vol. 56, no. 3, pp. 277–299, 2009.

[9] L. Birglen, C. Gosselin, and T. Laliberté, Underactuated robotic hands, ser. Springer Tracts in Advanced Robotics. Springer Verlag,2008, vol. 40.

[10] C. M. Gosselin and T. Laliberté, "Underactuated mechanical finger with return actuation," USA Patent 5,762,390, June 9, 1998.

[11] T. Laliberte, L. Birglen, and C. Gosselin, "Underactuation in robotic grasping hands," Machine Intelligence & Robotic Control, vol. 4, no. 3, pp. 77–87, 2002.

[12] M. Ciocarlie and P. Allen, "A constrained optimization framework for compliant underactuated grasping," Mechanical Sciences, vol. 2, no. 1, pp. 17–26, 2011.

[13] A. Jafari, N. G. Tsagarakis and D. G. Caldwell " Exploiting natural dynamics for energy minimization using an Actuator with Adjustable Stiffness (AwAS)" in the proceeding of IEEE International Conference on Robotics and Automation (ICRA) 2011, pp. 3561-3569.